Light Metals 2014
Edited by: John Grandfield
TMS (The Minerals, Metals & Materials Society), 2014

TEXTURE ANALYSIS OF ANODE PASTE IMAGES

Julien Lauzon-Gauthier[1], Carl Duchesne[1], Jayson Tessier[2]
[1]Aluminium Research Center-REGAL, Chemical Engineering Department, Université Laval, Québec (Qc), Canada, G1V 0A6
[2]Alcoa Global Primary Metals, Center of Excellence, Deschambault (Qc), Canada, G0A 1S0

Keywords: Anode paste, image analysis, multivariate analysis, wavelet texture analysis

Abstract

An important issue for the anode manufacturers is the increased variability of the raw materials and its negative impact on baked anode quality. This variability could be reduced by timely corrective actions applied on selected manipulated variables at the green mill (i.e. process control). However, the lack of rapid sensors for measuring anode quality is an important limitation to implementing feedback/feedforward control. Weekly averages of lab measurement are available too late to be used for feedback control. This work investigates the use of machine vision for sensing paste properties. The effects of changes in pitch demand of the aggregate and its particle size distribution, and mixing temperature on the visual appearance of laboratory paste image were studied. The 2D discrete wavelet transform (2D-DWT) was used to extract textural features for each image, followed by their analysis using Partial Least-Squares regression (PLS). Preliminary results show that the imaging sensor is sensitive to variations in pitch demand and aggregate size.

Introduction

Baked anode quality is an important issue for the primary aluminum industry. First, baked anode properties are affected by the declining quality and increasing variability of both anode raw materials (coke and pitch), and also by the frequent coke supplier changes made to meet process constraints and reduce cost. Fluctuations in baked anode quality can have an important impact on the performance of the reduction process, such as decreasing the energy and the current efficiency, increasing specific carbon consumption, increasing labor productivity and greenhouse gas emissions.

However, the baked anode quality control scheme currently used in the industry is not adequate to efficiently respond to the increased raw material variability. Generally, it is based on monitoring weekly averages of key properties measured by laboratory testing of anode core samples. These properties include mechanical, electrical, physical and chemical analyses, measured on less than 1 % of the total weekly production. Hence, core results may not be representative of the anode population. Furthermore, the results of core sample assays are typically available four weeks after the anodes are manufactured. Raw material properties are also obtained with significant delays for similar reasons. It is therefore not currently possible to implement corrective actions to the process at an early stage. Therefore, process deviations are typically detected a few weeks after the anodes have been produced.

There is a need for developing new sensors to measure and track variations in raw material properties and process operation at different stages within the carbon plant. Using those on-line sensors in a control system would help reducing the impact of raw materials variations on green and baked anode properties. One of the options explored in this work is the use of machine vision for rapid and non-destructive monitoring of the anode paste visual appearance which is known to be affected by raw material properties (coke in particular), formulation and mixing conditions (e.g. under or over-pitching leads to a dryer or wetter paste). In addition, the paste is an intermediate product that could allow early corrective actions to be implemented to formulation, for instance. To prove the concept, paste sample were produced in the laboratory to test the impact of paste formulation and processing conditions on its visual appearance. Variations in the pitch demand and size distribution of the dry aggregate mix were simulated. Pitch demand is defined as the amount of pitch required to achieve an optimum baked anode density given a certain coke source and size distribution [1]. This can be affected by many different factors in the paste formulation, such as coke porosity, amount of pitch, binder viscosity and so on.

This paper presents the work done using paste made in the laboratory. Lab paste was used instead of industrial paste to allow testing a wider range of variations under controlled conditions. This preliminary work focuses on understanding the impact of dry aggregate properties, formulation and mixing conditions on the paste visual appearance, and assessing the sensitivity of imaging sensor.

Experimental

Raw materials

One goal of this experiment was to reproduce the formulation of an industrial paste as closely as possible. For this reason, the aggregate mix formulation was based on ratios of classified raw material typically used at an industrial carbon plant instead the usual laboratory paste composition (i.e coke and pitch only). The dry aggregate contained the three coke fractions classified by their particle size (i.e. coarse, intermediate and fines) and the recycled butts. The latter are often omitted in lab formulations due to difficulties in obtaining a small but representative butt sample from a broad size distribution. Typically, the maximum particle size used is between 4 to 8 mm [2,3]. Very large particle can increase the variability in the laboratory paste due to the high relative importance of individual large particle in the small sample. In spite of these difficulties, it was decided to keep them in the formulation in order to mimic industrial paste. All of the fractions were sampled from classified material from storage silos. Finally, solid pitch was used. The raw materials came from the Alcoa Deschambault carbon plant. Only the recycle green scrap was omitted in the paste formulation.

Design of experiments

A total of 21 different mixes were prepared to simulate a wide range of variations in the dry aggregate pitch demand and size distribution across the various paste samples. A few replicates

were made for some mixes for a total of 30 paste samples to be imaged and analyzed.

Expected effects of the different experiments

The changes made to the base case mix were either aimed at changing the dry aggregate pitch demand or modifying its size distribution. The 21 paste mixes prepared in the lab are listed in Table I. The symbols identifying each mix will be used in the results section. The percentages for the coarse, intermediate, fines and butts fractions are given on a dry aggregate basis, but the pitch % is given on the paste weight basis.

Table I – Description of experimental paste mixes

Description	*Name*	*Symbol*
Base mix	base	●
Increased butts ratio	B_-10%	■
Decreased butts ratio	B_+10%	■
Different Blaine number (fines fraction)	BL_2300	▼
Different Blaine number (fines fraction)	BL_4000	▼
Different Blaine number (fines fraction)	BL_6000	▼
Decreased fines ratio in the aggregate mix	F_-4%%	+
Decreased fines ratio in the aggregate mix	F_-2%%	+
Increased fines ratio in the aggregate mix	F_+2%%	+
Increased fines ratio in the aggregate mix	F_+4%%	+
Decreased pitch ratio in the paste	P_-1.4%	★
Increased pitch ratio in the paste	P_+1.6%	★
Increased coarse and intermediate frac.	SD_+C+I	×
Increased intermediate frac.	SD_+I	×
Decreased coarse and intermediate frac.	SD_-C-I	×
Decreased intermediate frac.	SD_-I	×
Substitution of coarse frac. by shot coke	shot_20%	▲
Substitution of coarse frac. by shot coke	shot_40%	▲
Substitution of coarse frac. by shot coke	shot_60%	▲
Decreased mixing temperature	T_158°C	◆
Increased mixing temperature	T_188°C	◆

Different types of changes were made to the base case mix to modify the pitch demand of the dry aggregate. First, a ±10% change was made to the butts ratio. The change in the dry aggregate weight was compensated by adding/removing some of the coarse fraction. The butts are less porous than fresh coke particles. Thus, they need less pitch to wet them properly. High butts fraction should lead to wetter paste (for the same amount of pitch). Secondly, the Blaine number (BN) of the fines was varied. Different coke fines with specific fineness were prepared at the laboratory and used in substitution of the industrial fines fraction. The BN of the samples were measured using a Malvern laser diffraction particle size analyzer. Ball mill fines with 2300 4000 and 6000 BN where used. Finer fines (i.e. higher BN) should require more pitch because of the increased specific area. Hence, the paste should look dryer when using higher BN fines and wetter when using lower BN fines if the amount of pitch remains unchanged. Third, the fines ratio was modified and compensated by adding/removing coarse, intermediate and butts particles in equal amounts. The tested fines ratios were ±2 and ±4%. The more fines for a given amount of pitch, the dryer the paste be. Fourth, the pitch ratio was varied. There should be a direct relationship between the amount of pitch and the wetness of the paste. Fifth, a proportion of the coarse fraction was substituted with shot coke (e.g. 20, 40 and 60% of the coarse fraction). Because shot coke is typically less porous, the paste should look wetter when a greater amount of shot coke is added to the mix for the same amount of pitch. Finally, the mixing temperature was varied from 158 to 188 °C. When the temperature is too low, the pitch is more viscous and should not penetrate as much in the pores of the particles, leading to a wetter paste

The dry aggregate size distribution was varied by either substituting the coarse and intermediate fractions or the intermediate fraction only by the fines fraction (e.g. +10% coarse, + 5% inter and -15% fines or – 10% inter and + 10% fines). Although changes in the aggregate size distribution may also cause changes in pitch demand, it is expected that variations in aggregate size should have a different impact on paste visual appearance (i.e. its texture) than that of a change in pitch demand. Hence, the two types of disturbances should be distinguishable by the machine vision system.

Pre-heating and mixing

The paste samples were prepared in an industrial dough mixer fitted inside a laboratory oven. This set-up allowed good control on the pre-heating and mixing temperature.

Each constituent of the paste was weighted individually for every prepared sample. The total paste sample weight was 450 g. The four fractions of the dry aggregate were pre-heated over night in the mixing oven. The pitch was added to the mix and an additional pre-heating period of 30 min followed to let the pitch melt. Then the paste was stirred for 10 min. The standard mixing temperature was set to 178°C. When the mixing step was completed, the paste was spread in an aluminium container for the imaging step.

Imaging set-up

The imaging set-up for this experiment is shown in Figure 1. It consists of an Allied Vision Technologies Prosilica GX 6 megapixel color camera with a 50 mm Kowa lens, two 4.5 W LED light bulbs and Fresnel lenses to ensure uniformity of lighting. This set-up allows for a wide variety of adjustment of the lighting angle and camera height.

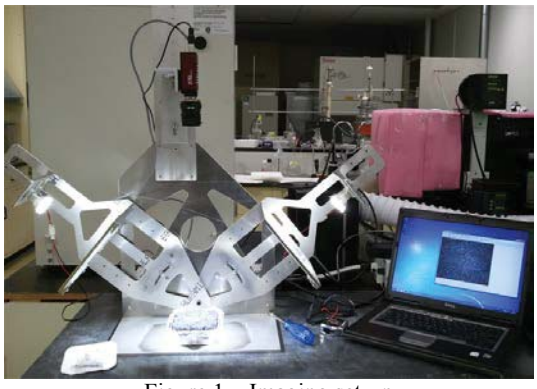

Figure 1 – Imaging set-up

Two images of each paste sample were taken to assess variability due to sampling. The paste was first poured in an aluminium container and imaged. Then the paste was put back in the mixing bowl, given a small hand mixing and poured again in the sample container. A second image was then captured. A set of 60 different paste images were available for texture analyses (i.e. 30 paste samples × 2 images/sample).

Machine vision approach for texture analysis

Image texture analysis

Image texture can be defined as a function of the spatial variation in pixel intensities [4]. Furthermore, this function can be established at different scales within the images (i.e. resolutions or levels of scrutiny). For example, high frequency variations from pixel-to-pixel yields a fine texture whereas lower frequency variations leads to coarser textures. Anode paste images are well suited for such a texture analysis because it is formed by a mixture of solid particles of different sizes and a viscous binder leading to a variety of textures (from fine to coarse and from smooth to rough) depending on the formulation (pitch ratio and aggregate size distribution).

The 2-Dimensional Discrete Wavelet Transform (2D-DWT) was used for extracting (i.e. quantifying) paste image textural features. This is a state-of-the-art multi-resolution textural method developed in the image processing field. The first step of the approach consists of selecting a waveform, also called mother wavelet, which shape roughly matches that of the image signals (i.e. pixel-to-pixel intensity variations in a given direction). Several wavelet families exist in the literature and, in general, the choice is not unique as many wavelets perform equally well on a given set of images. As opposed to the sine or cosine waves used in Fourier Transform, the wavelets have a finite length. This enables spatial-frequency decomposition of the image signals, a distinctive advantage over Fourier Transform which performs frequency decomposition only.

The mother wavelet can be dilated in order to capture information at different (decreasing) frequencies. This is modulated by a scaling coefficient which is an integral part of the wavelet equation. The wavelet at a given scale (i.e. value of the wavelet coefficient) is then convoluted with the image signals in the horizontal, vertical and diagonal directions. Having a finite length, the wavelet is translated across the image in all three directions (hence it captures spatial information), and the fit (i.e. correlation) between the wavelet and the image signal is computed for every pixel. The fit is represented by so-called detail coefficients. The output of 2D-DWT at scale *s* is a set of three detail subimages D_s^H, D_s^V, D_s^D representing the information captured by the wavelet in all three directions at scale *s*. The procedure is then repeated for a selected number of scales (*s*=1,2,…S). Note that the 2D-DWT can also be viewed as a filtering approach where the detail subimages contain band-pass information at different frequency ranges (i.e. scales). Since the scale is inversely proportional to frequency, the detail subimages at the first scale will capture high frequency information, or small size features (fine textures), whereas higher scales will contain lower frequency information (coarser objects or textural features). After filtering the image at a selected number of scales, the residual image is called the approximation subimage. The 2D-DWT approach is usually made robust to noise (high frequency) and lighting variations (low frequency) by leaving the first detail and approximation subimages out of subsequent analyses. Interested readers are referred to Mallat [5] for more details on the method.

To analyze and compare the texture of different images, it is a common practice to compute a row vector of scalar textural descriptors from the detail subimages (D_s^H, D_s^V, D_s^D, *s*=1,2,..S) and collecting them in a matrix for further analyses, such as classification or regression against responses of interest. The reader is referred to Duchesne et al. [6] for a good review on this topic. The energy of each detail subimage was used as textural descriptors in this analysis. The energy is a measure of the variance of the detail coefficients at each decomposition level. Alternatively, it can be interpreted as the amount of signal at a given frequency range (scale) contained in an image. The energy E is defined in the equation below, where D_s^k is the detail subimage of size (*m,n*) at scale *s*, and k=H,V,D (direction). The energy of each detail coefficients is normalized by the number of pixel in the original image of size (*M,N*).

$$E_s^k = \frac{\sum_{i=1}^{m}\sum_{j=1}^{n}\left\{D_s^k(i,j)\right\}^2}{M \times N} \quad (1)$$

Note that the DWT algorithm performs dyadic down-sampling (decimation) of the image at each scale rather than dilating the mother wavelet, which length is kept constant. That is, the size of the detail subimages D_s^k (m,n) in eq. 1 decrease by a twofold factor at each scale. This is very computationally efficient, but imposes a constraint on the frequency resolution of the approach. Other wavelet methods, such as wavelet packets and the continuous wavelet transform can improve frequency resolution but were not tested at this point.

Datasets

The data collected from the image analysis are divided in two data matrices. The first, called the design matrix (**X**), contains information on the paste formulation (Table II). The second, called the image features matrix (**Y**), contains the extracted image features. These are the energy of the 21 detail subimages computed on 7 scales (i.e. 3 subimages/scale) using the *symlet4* mother wavelet. The variables in this dataset are labeled by the direction of the detail coefficient as well as its level of decomposition. The higher the scale, the lower the frequency associated with it.

Table II – Design dataset variables

Variable number	*Variable name*
1	Coarse (%)
2	Inter (%)
3	Fines (%)
4	Butts (%)
5	Pitch (%)
6	Pitch/Fines ratio
7	Shot in coarse faction (%)
8	Mixing Temperature (°C)
9	Blaine number

Multivariate analysis of image textural features

The image textural features were then analyzed using Partial Least-Squares (PLS) regression. The latter is a multivariate regression technique dealing with correlated data in both **X** and **Y**. Some of the variables in the design data matrix (Table II) are correlated to a certain extent because the changes in some dry aggregate fractions were compensated by changes in other fractions. The image features are also collinear to some extent. The PLS model structure is shown by eq. 2-5. It performs a bilinear variance-covariance decomposition of the **X** and **Y** data

(eq. 2-3) by finding a small number of orthogonal linear combinations of the **X**-variables that are the most predictive of (i.e. correlated with) the **Y** variables (eq. 4). These combinations, also called principal components, and stored in the columns of the weight matrix **W*** (eq. 4), define a lower dimensional subspace in both data spaces. The column vectors in the **P** and **C** matrices are called loading vectors and define the subspaces that best represent **X** and **Y**, respectively. Projection of the **X** and **Y** data onto their respective subspaces yields the score vectors, the columns of **T** and **U**. The **E** and **F** matrices contain the PLS model residuals. The linear relationship between both spaces through their score vectors is defined by eq. 5, where **H** contains the residuals of that relationship. The components of the PLS model are ordered in such a way that the first component is the one that explains the greatest amount of covariance between **X** and **Y**, the second explains the greatest amount of covariance orthogonal to the first component, and so on. Several criteria are available for choosing the number of PLS components (*A*). We selected *A* so as to maximize the model predictive ability on the **Y** data. For more details on PLS, the reader is referred to [7].

$$\mathbf{X} = \mathbf{T}\mathbf{P}^{\mathrm{T}} + \mathbf{E} \quad (2)$$

$$\mathbf{Y} = \mathbf{U}\mathbf{C}^{\mathrm{T}} + \mathbf{F} \quad (3)$$

$$\mathbf{T} = \mathbf{X}\mathbf{W}^{*} \quad (4)$$

$$\mathbf{U} = \mathbf{T} + \mathbf{H} \quad (5)$$

To interpret the model and the information contained in the data, it is common practice to look at different types of plots. The scatter plots of pairs of scores (e.g. $\mathbf{t_1}$-$\mathbf{t_2}$ or $\mathbf{u_1}$-$\mathbf{u_2}$) show the clustering patterns of the observations (i.e. design data or image features associated with each paste sample). Scatter plots of the loadings for pairs of components (e.g. $\mathbf{w_1c_1}$- $\mathbf{w_2c_2}$ plots) allow for interpreting the relationships between the **X** and **Y** variables. Other plots are also used in practice but not shown in this paper (refer to [7] for more details).

Results

Some hurdles

The small size of the paste samples was an important issue in these experiments. The dry aggregate fractions were stored in 20-25 kg buckets. But only 60 g to 125 g of each constituent was needed for a paste sample. It was very difficult to obtain a representative size distribution for each dry aggregate fraction.

The recycle butts fraction contains a very large distribution of particle size (i.e. from 2-3 cm to a few µm). For this fraction in particular, the full industrial sample was split into several smaller fraction of approximately 100 g using a sample splitter and than the 4 corners method on a large sheet of paper. Even with careful manipulations, it was not possible to obtain a constant size distribution in all split fractions. This is illustrated in Figure 2, where the size distribution for 5 split butts sample is shown. There is a large variability of the larger particles in the samples.

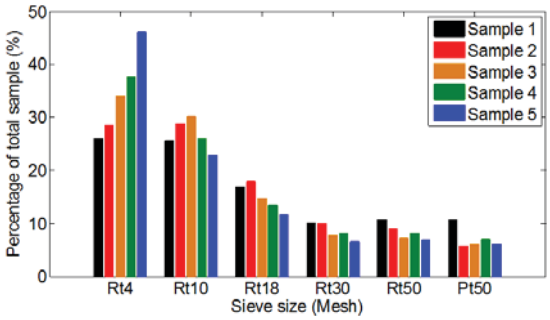

Figure 2 – Butts size distribution span

Image analysis results

Table III shows the percentage of variance of **X** and **Y** explained by the PLS model. The model captures 59% of the variability in the image features in spite of the variations introduced by sample preparation.

Table III – Percentage of variance explained by the PLS model for the first two principal components

	Design-Block **(X)**		Image features-Block **(Y)**	
Comp	This (%)	Total (%)	This (%)	Total (%)
1	30.44	30.44	47.42	47.42
2	12.36	42.80	11.45	58.87

Figure 3 displays the latent variable score space for the two components PLS model. This score plot represents the main direction of variability in the datasets. Each marker represents one experiment. It is possible to look at the clustering patterns (i.e. similarity or differences) between all the paste samples by looking at their projection in the LV space. Arrows indicates the phenomena that the experiment was designed to stimulate (i.e. change in pitch demand in blue and size distribution in green). The upper right and lower left corners represents the regions where the paste is wetter and dryer respectively. This was validated by observations made on the paste visual appearance. The orthogonal direction indicated by the green arrow is related with the size of the dry aggregate within the paste samples. This figure is representative of the experimental design chosen for the paste samples.

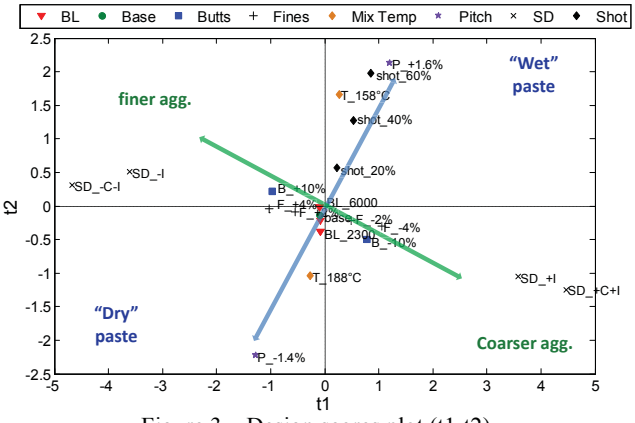

Figure 3 – Design scores plot (t1-t2)

It is also possible to look at the latent variable space for the image features dataset. These results are shown in Figure 4. Again, the

two arrows indicate the two main effects studied. This is a very important figure for the analysis of the results and it will be commented further in the next few paragraphs.

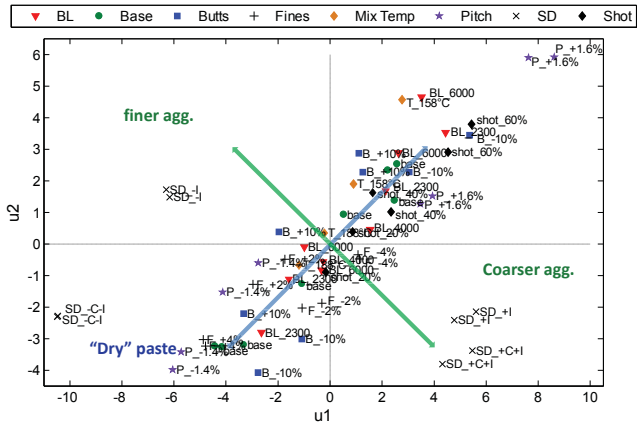

Figure 4 – Image features scores plot (u1-u2)

The results clearly show that increasing pitch content from -1.4 to +1.6% for the same dry aggregate drives the paste appearance from dry to wet. This experiment mimics under- and over-pitching situations and, without knowing what the optimum pitch level is for this aggregate, the proposed approach seems promising for detecting such situations. Changing the fines ratio also moves the paste visual appearance along the pitch demand direction (blue line in Figure 4). The paste sample with +4% fines falls in the dry paste region. Decreasing it to -4% brings paste image features close to the origin of the plot where the paste samples look wetter. This behavior is consistent with process knowledge. Increasing the amount of shot coke with respect to the base case leads to progressively wetter paste as shot coke is less porous and the amount of pitch is unchanged. The reader is reminded that these changes in shot coke are only a mean for modifying the dry aggregate porosity. Finally, increasing mixing temperature from 158-188ºC changes the paste appearance from wet to dry. The lower pitch viscosity at higher temperature should increase pitch penetration in the coke particles and hence, the paste would like dryer for the same aggregate and formulation.

The results obtained after varying the butts ratio and Blaine Number (BN) also drive the paste visual appearance along the pitch demand direction (dry-wet paste) as shown in Figure 4, but the interpretation is not as clear as with other experiments. Increasing butts ratio should move the paste sample towards the wetter region since, in general, the butts are less porous. Although most samples at +10% butts are in the wetter region and most samples at -10%% butts are in the dryer region, one sample at each of these conditions fall in the opposite quadrants. For BN, it was expected that higher BN fines should make the paste look dryer than with lower BN fines because the higher surface area of the fines should increase pitch demand. However, the paste samples with different BN are spread along the pitch demand direction. At this point, the reason for this is unknown. However, as mentioned earlier, sampling issues with butts and fines makes it difficult to ascertain what really was in the dry aggregates with respect to these two fractions. This sampling issue also probably contributed to the high variability of the base mix paste which is broadly spread along the pitch demand direction. In addition, as changes in certain fractions were compensated by changes in other fractions to maintain total dry aggregate weight, some of the effects might be confounded. Future work will look at resolving these issues.

Figure 4 also shows that the machine vision approach is also sensitive to changes in aggregate size distribution, and the latter can be distinguished from variations in pitch demand. The experiments made to change the dry aggregate size distribution moved the paste sample appearance along the orthogonal direction from pitch demand (i.e. green direction in Figure 4). The paste with less intermediate size coke (i.e. SD_-I) is situated in the upper left quadrant, while the coarser pastes (i.e. SD_+C+I and SD_+I) are located in the lower right quadrant. Similar results are observed with the finer formulation past (i.e.SD_-C-I). Their position in the bottom left corner indicates that the high content of the fines affected the pitch demand at the same time as the size distribution.

The loadings biplot shown in Figure 5 is used to interpret the correlation between the design variables and the image features. It can be used simultaneously with Figures 3 and 4. The directions of changes are the same in the three plots. In the pitch demand direction the energy of the detail coefficients increases in all decomposition levels when the wetness of the paste increases. For the size distribution the energy of the decomposition levels 1 to 4 (i.e. higher frequencies) increases faster than the decomposition levels 5 to 7 when the formulation of the paste is coarser.

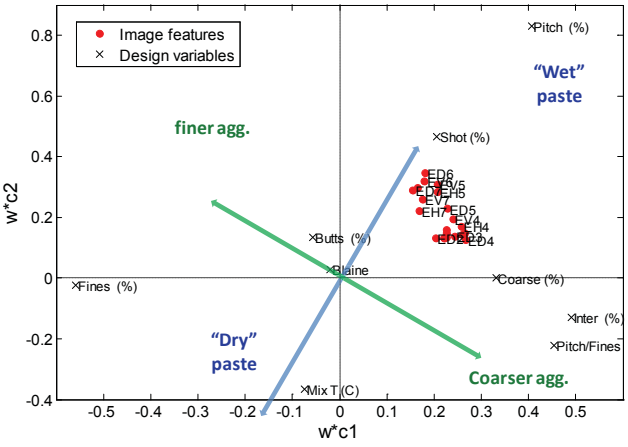

Figure 5 – Loadings bi-plot (w*c1 – w*c2)

The wetness of the paste is correlated with the overall energy of the images since all the detail coefficient energy change in a similar manner. The total energy of a wet paste is higher than the total energy of a dry paste. To better understand the differences, the paste with the highest energy (P_+1.6%) and the lower energy (SD_-C-I) are shown in Figure 6. They correspond to the paste with the most pitch and the paste with the finest formulation. Wetter pastes have more specular reflection (i.e. more glossy images) which leads to higher overall energy.

For the size distribution direction, the additional specular reflection due to the pitch demand is also visible in the mix with lower fines content (i.e. coarser mix). But there is an additional effect that changes the variations of the energy in the decomposition levels 5 to 7. The pastes with a higher (SD_+I) and lower (SD_-I) intermediate formulation are shown in Figure 7.

a) 

b) 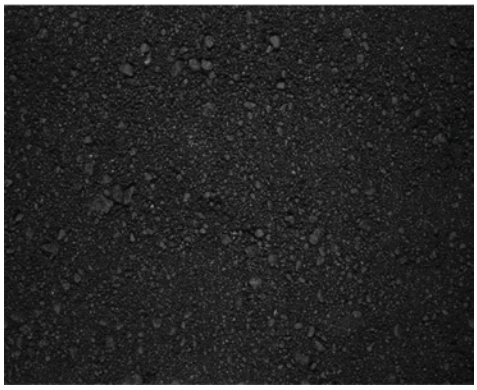

Figure 6 – images of paste sample showing variations in pitch demand: a) wetter paste (P_+1.6%) and b) dryer paste (SD_-C-I)

a) 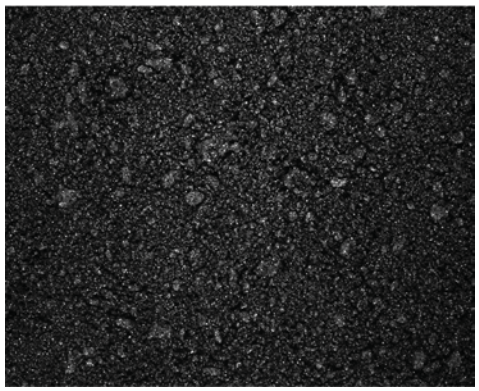

b) 

Figure 7 – images of paste sample showing variations in size distribution: a) coarser mix (SD_+I) and b) finer mix (SD_-I)

Conclusion

The hypothesis of this work was that the anode paste appearance changes as a function of pitch demand and size distribution of the dry aggregate. This change in visual appearance can be detected using a texture analysis method applied on paste images. It was possible to discriminate between the dry aggregate formulations and the pitch demand variations. Future work should concentrate on validating the robustness of this method on industrial paste.

Acknowledgments

Authors would like to acknowledge the financial support of the Natural Sciences and Engineering Research Council of Canada (NSERC) and Alcoa. A part of the research presented in this paper was financed by the *Fonds de Recherche du Québec-Nature et Technologies* (FRQ-NT) by the intermediary of the Aluminium Research Centre-REGAL. Special thanks to Kamran Azari Dorcheh for the help in the sample preparation and Alcoa for the raw materials and permission to publish this paper. The first author would like to acknowledge the financial support of Rio Tinto Alcan through its graduate scholarship program.

References

1. Hulse, K. L. et al. “Process Adaptations for Finer Dust Formulations: Mixing and Forming”. In *Essential Readings in Light Metals*; Tomsett, A.; Johnson, J., Eds.; John Wiley & Sons, Inc., 2013; pp. 322–327.

2. Fischer, W. K.; Mannweiler, U.; Kelle, F.; Perruchoud, R. C.; Bühler, U. *Anodes for the aluminium industry*; R & D Carbon Ltd., 1995.

3. Azari, K. et al. Mixing variables for prebaked anodes used in aluminum production. *Powder Technol.* **2013**, *235*, 341–348.

3. Tuceryan, M.; Jain, A. K. “Texture Analysis”, in: C.H. Chen, L.F. Pau, P.S.P Wang (Eds.), *The Handbook of Pattern Recognition and Computer Vision*, *2nd edition,* World Scientific Publishing Co, 1998, 207-248

5. Mallat, S. G. “A theory for multiresolution signal decomposition: the wavelet representation”. *Pattern Anal. Mach. Intell. IEEE Trans.* **1989**, *11*, 674 –693.

6. Duchesne, C.; Liu, J. J.; MacGregor, J. F. “Multivariate image analysis in the process industries: A review”. *Chemom. Intell. Lab. Syst.* **2012**, *117*, 116–128.

7. Wold, S.; Sjöström, M.; Eriksson, L. “PLS-regression: a basic tool of chemometrics”. *Chemom. Intell. Lab. Syst.* **2001**, *58*, 109–130.